Aalborg Universitet

AALBORG UNIVERSITY DENMARK

A Novel Lens Antenna Design Based on a Bed of Nails Metasurface for New Generation Mobile Devices

Paola, Carla di; Zhao, Kun; Zhang, Shuai; Pedersen, Gert Frølund

Published in:
2020 14th European Conference on Antennas and Propagation (EuCAP)

DOI (link to publication from Publisher):
10.23919/EuCAP48036.2020.9135354

Publication date:
2020

Document Version
Accepted author manuscript, peer reviewed version

A Novel Lens Antenna Design Based on a Bed of Nails Metasurface for New Generation Mobile Devices

Carla Di Paola[1], Kun Zhao[1,2], Shuai Zhang[1], Gert Frølund Pedersen[1]
[1]Department of Electronic Systems, Aalborg University, Denmark, {cdp, kz, sz, gfp}@es.aau.dk
[2]Research Center Lund, Sony Corporation, Lund, Sweden

***Abstract*—This paper presents a lens antenna concept with multibeam performance in the mm-wave band for the next generation mobile devices. The lens consists of metallic vias, etched in the substrate with different height, to obtain different permittivity. The goal is to correct the phase distribution of the incoming electromagnetic wave, to radiate towards the desired direction with high gain. The -10 dB impedance bandwidth of 4 GHz is achieved around the central frequency of 38 GHz. Three beams pointing different directions allow to cover the angle range of 68° in azimuth with realized gain higher than 5 dBi. Simulations of the lens antenna placed on the top left corner of a mobile phone PCB confirm the performance of the prototype. Moreover, the total scan pattern (TSP) highlights wide coverage of 110° in elevation, where the gain is overall more than 6 dBi, reaching peak values of 9.4 dBi.**

***Index Terms*—Mobile terminal antenna, lens antenna, metasurface, multibeam antenna, 38 GHz.**

I. Introduction

The high speed data transfer required by the upcoming fifth generation mobile communication system (5G) cannot be satisfied by the conventional frequency bands. Therefore, centimeter-wave (cm-wave) and millimeter-wave (mm-wave) bands are selected in order to provide wider bandwidths, that support higher capacity and massive device connectivity and guarantee lower end to-end latency and better user experience [1]–[4]. However, by increasing the operating frequency, the free-space path loss becomes more significant than at the sub-6 GHz 4G bands, according to the Friis transmission equation [5].

Thus, high gain antennas are needed, in order to mitigate the free space attenuation [6]. Since high gain leads to narrow radiation beamwidth, antennas able to form multiple beams in different direction, reconfiguring their radiation patterns in real time [7], are needed to achieve a large beam steering range. Therefore, beam-steerable directional phased arrays result good candidates, thanks to their property to realize beam forming and obtain the desired coverage, for both the base station and the mobile device of the emerging 5G systems, as reported in [8]–[10]. Nevertheless, phased antenna arrays, despite their ability to shape and adjust the radiation pattern electronically, present bandwidth limitations, since phase shifters do not provide the correct rate of change of phase with frequency, to guarantee the same beam pointing over a wide bandwidth [11]–[13]. Moreover, they are responsible of the increased insertion loss of the entire structure.

Alternative beamforming networks (BFNs) are based on circuit or quasi-optics techniques. The first require delay lines and couplers, and their main representative is the Butler matrix [14]–[16]. Characterized by a compact layered topology and a wide achievable bandwidth, this feeding network suffers, though, from high loss. Quasi-optic techniques employing a lens aim to obtain size reduction and guarantee low profile, low cost and high performance. On the other hand, this BFN is affected by narrow band, as demonstrated in the research works in [17]–[20]. However, the BFN featuring the lens is one of the most promising low cost solutions for high frequency and highly directive antennas, ensuring low circuit complexity and lower loss compared to the other solutions mentioned above [21]. Lenses are exploited to modify the amplitude and the phase of the electromagnetic waves arriving from the sources, changing thus the field distribution at the aperture of the antenna, with the goal to obtain the desired beam pointing.

State of the art optically transformed lenses are ideal candidate for the design of highly directive antennas. Realized ad hoc for a specific feeding, hence the name bespoke lenses, they allow better radiation performance compared to homogeneous lenses [22], though their implementation in 3D will be made possible and affordable in the future, thanks to the development of 3D printers, which exploit low-loss dielectric materials.

Two-dimensional lenses, characterized by parallel plates with different dielectric materials inside, are then preferred, even though limited by the number of materials commercially available. This problem is overcome in [23]–[26] by drilling holes with different diameter and density or modifying also the thickness of the dielectric material, in order to obtain larger number of discrete levels of permittivity.

Planar lenses can also be realized with metasurfaces at a low manufacturing cost. Metasurfaces give the opportunity to realize fully metallic lenses, which have lower losses than dielectrics at higher frequencies. However, the narrow band of operation represents a limitation to their implementation. Higher symmetries have been demonstrated to generate low-dispersive unit cells [27], which allow to realize planar lenses with ultrawideband properties [28], [29]. The most common configurations for metasurfaces are periodic arrays of patches or holey metallic surfaces placed over a dielectric slab [30] and the bed of nails [31].

A novel lens design for mobile handset application, based on the second configuration, is presented in this paper. A bed of nails is employed in order to map the excitation fields originated from the feeding ports to the desired amplitude and phase distributions at the input of the radiating elements. This is accomplished by using groups of metallized vias etched in the PCB with different height, in order to modify the refractive index of the substrate. A parallel plate resonator placed on both sides of the PCB is selected as the matching layers for the lens antenna. It allows a -10 dB impedance bandwidth of 4 GHz, around the central frequency of 38 GHz, relatively wide for a lens antenna of this kind. The possibility to implement the proposed prototype on a PCB substrate with small thickness makes it feasible for mobile handset application. Moreover, the small clearance of less than 3 mm fulfils one of the requirements of the new generation mobile devices. Three beams with different directions can be generated to cover the angle range wider than 60° with gain higher than 5 dBi.

The paper is organized as follows. The main parts of the proposed lens antenna are described in detail in Section II. In Section III, the analysis conducted on the simulated structure is presented and discussed. The performance of the prototype placed in the corner of the mobile phone PCB are commented in Section IV. Finally, Section V concludes the paper.

II. Structure of the Lens Antenna

Figure 1 shows the design of the proposed lens antenna. Implemented in a substrate with dielectric constant $\varepsilon_r = 2.805$, width $W = 26$ mm, length $Hl + Hc = 19.4$ mm and thickness $T = 1.5$ mm, coated on both sides by a layer of copper, it consists of three main parts.

The first is the feeding region. Three waveguide ports are selected for the numerical study conducted using the electromagnetic simulator *CST Microwave Studio 2019*.

The following part is the beam forming network, the lens realized with the matasurface based on the bed of nails configuration. As reported in Fig. 1(b), it is a symmetric structure made up of metallic vias etched in the substrate, having the same diameter of 0.5 mm, the same center-to-center distance of 0.5 mm but different height, in order to get different value of permittivity. In particular, the central vias (red) are the highest, giving thus the highest permittivity, that decreases moving to the edges, where the vias are gradually shorter. In addition, another group of vias (brown), smaller than the red ones, is located in the center, in order to match the portion with the highest permittivity with the rest of the substrate with low permittivity. The dimensions are listed in Table I. This discretization, changing the propagation constant of the guided mode, allows to adjust the electromagnetic wave phase distribution at the input of the radiating elements, to direct the beam to the desired direction.

The matching layers, a parallel plate resonator with height $\lambda/4$, are placed in the last section corresponding to the small clearance $Hc = 2.4$ mm.

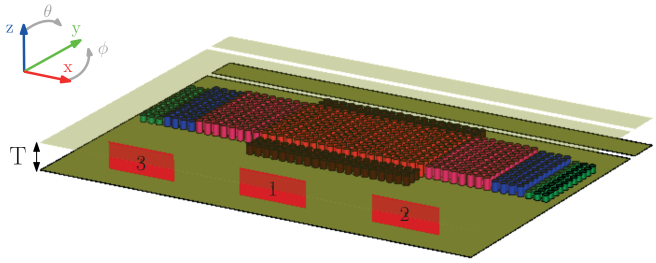

(a)

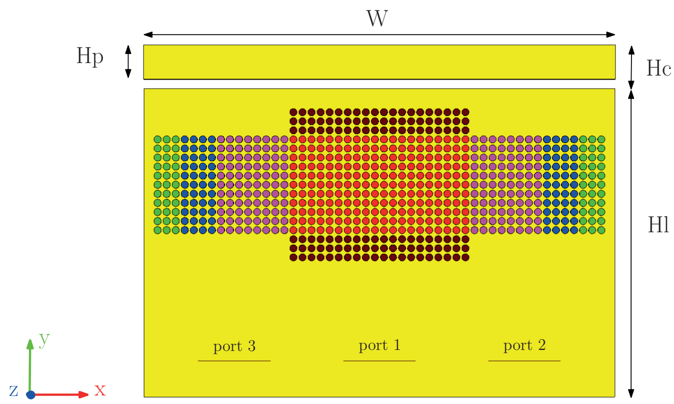

(b)

Fig. 1. (a) Perspective and (b) top view of the geometric structure of the proposed lens antenna for 5G mobile-phones. For a better view of the vias, the substrate is hidden and the metal layer on top is transparent.

Tab. I. Dimensions of the lens antenna parameters (units: mm).

Parameter	Value	Vias Color	Vias Height
T	1.5	red	0.72
W	26	pink	0.68
Hl	17	blue	0.56
Hc	2.4	green	0.35
Hp	1.9	brown	0.5

III. Lens Antenna Performance

The curves representing the S-parameter characteristics of the proposed lens antenna are reported in Fig. 2. The simulated -10 dB bandwidth is $35.6-39.6$ GHz around the central frequency of 38 GHz. In this interval S_{22} presents matching problems and, even though the value is not higher than -6 dB, it needs to be optimized, since it affects the realized gain. The mutual coupling between the ports 1 and 2 is due to the reflections inside the BFN. However, around 38 GHz it is below -15 dB.

The realization of the desired beam pointing, as introduced before, is accomplished by controlling the phase distribution of the electromagnetic wave through the etching of metallic vias in the substrate. In particular, as shown in Fig. 3, the high permittivity region created by the presence of the highest vias, allows to slower the spherical wave generated from port 1, obtaining a plane wave at the input of the radiating elements, with consequent radiation to the top. In the same way, the excitation field originated from port 2 is accelerated

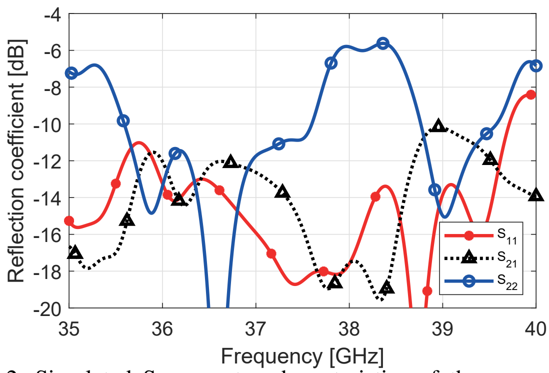

Fig. 2. Simulated S-parameter characteristics of the proposed lens antenna. Due to the symmetric structure, S_{33} and S_{31} are omitted here.

when encountering the area with lower permittivity, given by the shorter vias, and decelerated in the center, allowing the resulting plane wave to propagate to the left and the patches to radiate in the corresponding direction.

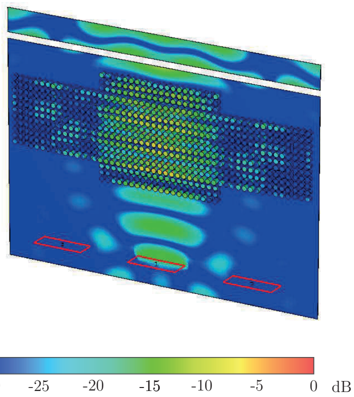

Fig. 3. Electric field distribution inside the proposed lens antenna at 38 GHz when port 1 is excited.

The effectiveness of the metallic vias is confirmed by the 3D radiation patterns generated at 38 GHz, shown in Fig. 4. They prove that the lens allows the electromagnetic waves originated at port 2 and 3 to be bended and radiate towards the opposite direction. In fact, the excitation from port 2 on the right produces a beam pointing to the left (Fig. 4(a)) and vice versa for port 3 (Fig. 4(c)). Moreover, the breaking effect played by the central vias, reducing the phase velocity of the spherical wave coming from port 1, results in the radiation directed to the top (Fig. 4(b)).

The three beams scan an angle range wider than 60° in azimuth, as highlighted by the envelope plotted in Fig. 5. In fact, at $\theta = 90°$, the beam is steered from 56° to 124° along ϕ with realized gain higher than 5 dBi. In particular, the first radiation scans the interval $70° < \phi < 110°$ with peak gain of 6.2 dBi at 77° and 103°. The second and third beam cover 14° each, reaching the maximum gain of 6.6 dBi at 62° and 118°. As expected, the main beam is very narrow at high frequency.

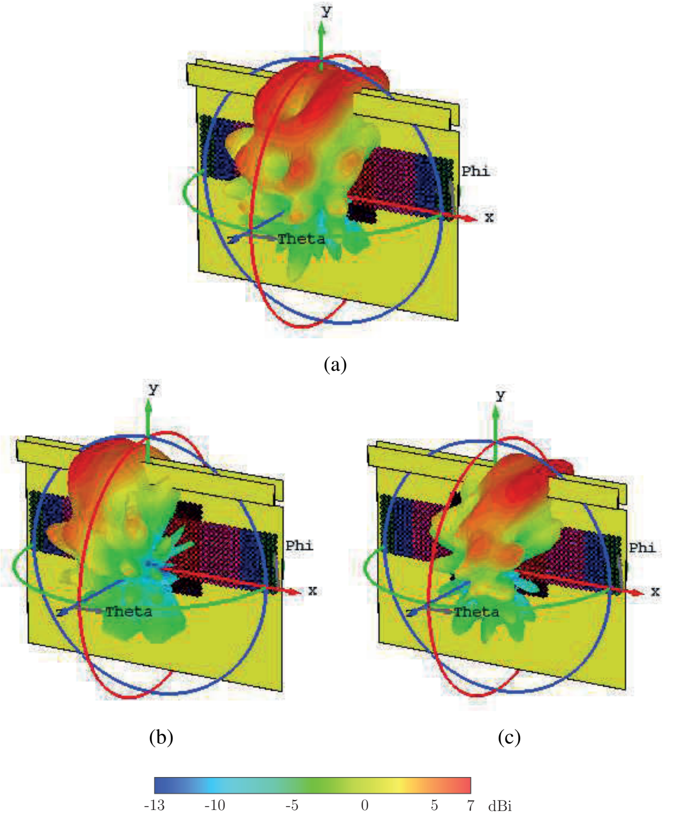

Fig. 4. Simulated 3D-radiation pattern of the lens antenna at 38 GHz when (a) port 2 (b) port 1 and (c) port 3 are excited.

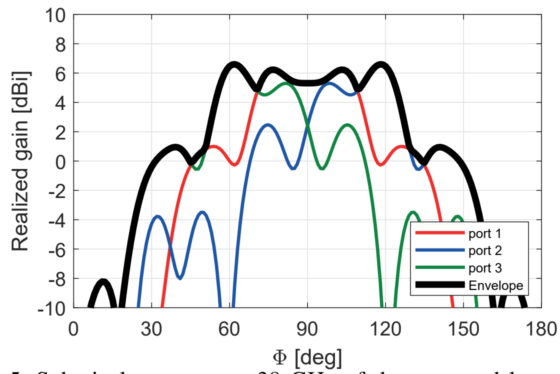

Fig. 5. Spherical coverage at 38 GHz of the proposed lens antenna evaluated at $\theta = 90°$.

IV. Integration in the Mobile Phone PCB

In order to prove the performance of the proposed lens antenna in a quasi-real scenario, simulations of the prototype placed on the upper left corner of the mobile phone PCB, as shown in Fig. 6, are performed with CST. The dimensions of the substrate are in accordance with a typical smart-phone form factor, i.e. width of 70 mm, and length of 130 mm.

In general, both the S-parameter characteristics and the radiation properties of the lens antenna are not affected by the presence of the substrate, as confirmed by the 3D-radiation patterns generated at 38 GHz, reported in Fig. 7. The plots highlight also the coverage in elevation. Regarding the central radiation in Fig. 7(a), the maximum gain along θ is observed when $\phi = 75°$ and symmetrically $105°$. In particular, realized gain higher than 6 dBi is evaluated in the interval $54° < \theta < 126°$. Examining the radiation patterns related to port 2 and 3, respectively in Fig. 7(b) and 7(c), the highest gain is reached in a smaller interval $63° < \theta < 117°$ and exactly at $\phi = 60°$ for port 3 and symmetrically $\phi = 120°$ for port 2.

Finally, the total scan pattern, being the 3-D envelope of the three individual patterns, allows a better understanding of the radiation performance of the lens antenna. Looking at Fig. 8, it is possible to state that the expected beam steering of $68°$ is obtained in azimuth, with corresponding $110°$ scanning in elevation. The realized gain is overall higher than 6 dBi, reaching the peak value of 9.4 dBi.

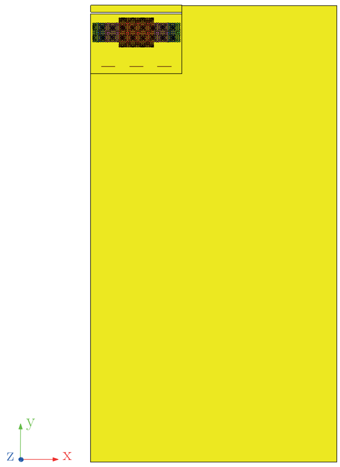

Fig. 6. Design of the proposed lens antenna placed in the corner of the PCB mobile phone.

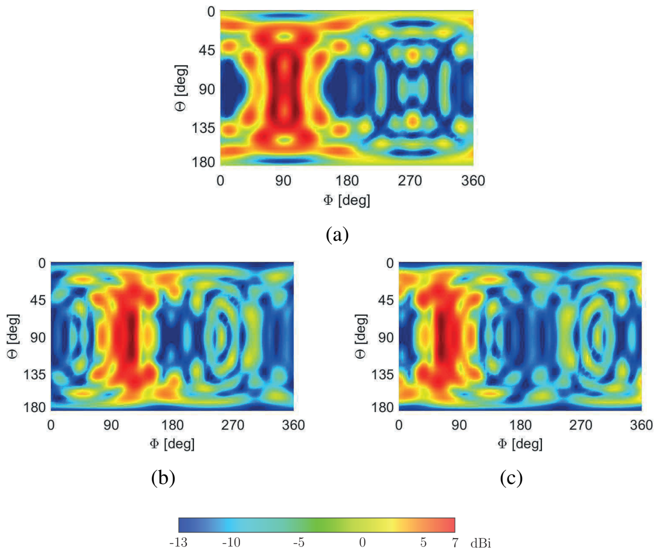

Fig. 7. Simulated 3D-radiation pattern of the lens antenna placed in the corner of the PCB mobile phone at 38 GHz when (a) port 1 (b) port 2 and (c) port 3 are excited. For ϕ varying from $0°$ to $360°$ the corresponding value along θ is plotted.

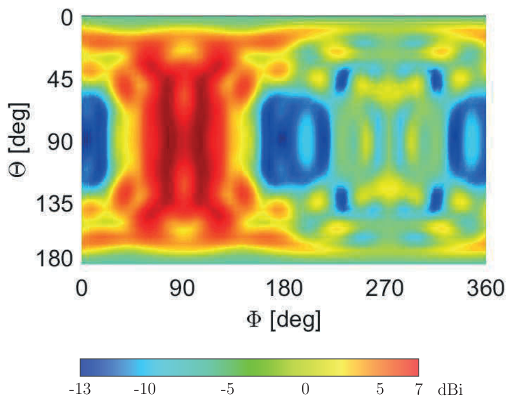

Fig. 8. Total Scan Pattern (TSP) of the lens antenna placed in the corner of the PCB mobile phone simulated at 38 GHz.

V. Conclusion

This work proposes a new lens antenna for the next generation beam steerable arrays. The main purpose of the design is to obtain multibeam performance in the mm-wave band and is achieved through the implementation of a lens, a metasurface based on the bed of nails configuration, and employing a parallel plate resonator as the matching layers. The goal of the lens, consisting of vias etched symmetrically in the substrate with different height, is to map the electromagnetic wave generated from the feeding ports to the desired amplitude and phase distributions at the input of the radiating elements, in order to obtain the desired beam pointing. In particular, in the configuration analyzed, three different excitations cover the angle range of $60°$ in azimuth with realized gain higher than 5 dBi at 38 GHz. The prototype can be implemented on a PCB substrate with small thickness, resulting a good candidate for mobile handset application. In fact, placing it on the top left corner of the mobile phone PCB, the performance are confirmed at the selected frequency. Future work aims to enhance the design, in order to improve the impedance matching and increase the realized gain. In addition, applying glide symmetry, it is possible to enlarge the bandwidth and adding more feeding ports allows to increase the number of beams. The following step consists in replacing the waveguide ports with coaxial cables and consequent realization of the prototype.

Acknowledgments

The work presented in this paper has been conducted under the framework of the RANGE project, supported by The Innovation Fund Denmark together with industry partners: WiSpry, AAC and Sony Mobile.

References

[1] Z. Pi and F. Khan, "An introduction to millimeter-wave mobile broadband systems," *IEEE communications magazine*, vol. 49, no. 6, 2011.

[2] T. S. Rappaport, S. Sun, R. Mayzus, H. Zhao, Y. Azar, K. Wang, G. N. Wong, J. K. Schulz, M. Samimi, and F. Gutierrez, "Millimeter wave mobile communications for 5g cellular: It will work!," *IEEE access*, vol. 1, pp. 335–349, 2013.

[3] T. Bai and R. W. Heath, "Coverage and rate analysis for millimeter-wave cellular networks," *IEEE Transactions on Wireless Communications*, vol. 14, no. 2, pp. 1100–1114, 2015.

[4] C.-X. Wang, F. Haider, X. Gao, X.-H. You, Y. Yang, D. Yuan, H. Aggoune, H. Haas, S. Fletcher, and E. Hepsaydir, "Cellular architecture and key technologies for 5g wireless communication networks," *IEEE Communications Magazine*, vol. 52, no. 2, pp. 122–130, 2014.

[5] C. A. Balanis, *Antenna theory: analysis and design*. John wiley & sons, 2016.

[6] S. Rajagopal, S. Abu-Surra, Z. Pi, and F. Khan, "Antenna array design for multi-gbps mmwave mobile broadband communication," in *Global Telecommunications Conference (GLOBECOM)*, pp. 1–6, IEEE, 2011.

[7] Z. Sipus and T. Komljenovic, "Multi-shell radially symmetrical lens antennas," in *Aperture Antennas for Millimeter and Sub-Millimeter Wave Applications*, pp. 37–73, Springer, 2018.

[8] W. Hong, K.-H. Baek, Y. Lee, Y. Kim, and S.-T. Ko, "Study and prototyping of practically large-scale mmwave antenna systems for 5g cellular devices," *IEEE Communications Magazine*, vol. 52, no. 9, pp. 63–69, 2014.

[9] W. Hong, Z. H. Jiang, C. Yu, J. Zhou, P. Chen, Z. Yu, H. Zhang, B. Yang, X. Pang, M. Jiang, *et al.*, "Multibeam antenna technologies for 5g wireless communications," *IEEE Transactions on Antennas and Propagation*, vol. 65, no. 12, pp. 6231–6249, 2017.

[10] W. Roh, J.-Y. Seol, J. Park, B. Lee, J. Lee, Y. Kim, J. Cho, K. Cheun, and F. Aryanfar, "Millimeter-wave beamforming as an enabling technology for 5g cellular communications: Theoretical feasibility and prototype results," *IEEE communications magazine*, vol. 52, no. 2, pp. 106–113, 2014.

[11] L. Stark, "Microwave theory of phased-array antennas — a review," *Proceedings of the IEEE*, vol. 62, no. 12, pp. 1661–1701, 1974.

[12] R. C. Hansen, *Phased array antennas*, vol. 213. John Wiley & Sons, 2009.

[13] D. Parker and D. C. Zimmermann, "Phased arrays-part 1: theory and architectures," *IEEE Trans. Microw. Theory Tech.*, vol. 50, no. 3, pp. 678–687, 2002.

[14] J.-W. Lian, Y.-L. Ban, C. Xiao, and Z.-F. Yu, "Compact substrate-integrated 4$\times$ 8 butler matrix with sidelobe suppression for millimeter-wave multibeam application," *IEEE Antennas Wireless Propag. Lett.*, vol. 17, no. 5, pp. 928–932, 2018.

[15] Y. Cao, K.-S. Chin, W. Che, W. Yang, and E. S. Li, "A compact 38 ghz multibeam antenna array with multifolded butler matrix for 5g applications," *IEEE Antennas Wireless Propag. Lett.*, vol. 16, pp. 2996–2999, 2017.

[16] L.-H. Zhong, Y.-L. Ban, J.-W. Lian, Q.-L. Yang, J. Guo, and Z.-F. Yu, "Miniaturized siw multibeam antenna array fed by dual-layer 8$\times$ 8 butler matrix," *IEEE Antennas Wireless Propag. Lett.*, vol. 16, pp. 3018–3021, 2017.

[17] J.-W. Lian, Y.-L. Ban, Z. Chen, B. Fu, and C. Xiao, "Siw folded cassegrain lens for millimeter-wave multibeam application," *IEEE Antennas Wireless Propag. Lett.*, vol. 17, no. 4, pp. 583–586, 2018.

[18] Y. Cheng, W. Hong, and K. Wu, "Design of a substrate integrated waveguide modified r-kr lens for millimetre-wave application," *IET microwaves, antennas & propagation*, vol. 4, no. 4, pp. 484–491, 2010.

[19] K. Tekkouk, M. Ettorre, L. Le Coq, and R. Sauleau, "Multibeam siw slotted waveguide antenna system fed by a compact dual-layer rotman lens," *IEEE Trans. Antennas Propag.*, vol. 64, no. 2, pp. 504–514, 2016.

[20] Y. S. Zhang and W. Hong, "A millimeter-wave gain enhanced multibeam antenna based on a coplanar cylindrical dielectric lens," *IEEE Trans. Antennas Propag.*, vol. 60, no. 7, pp. 3485–3488, 2012.

[21] O. Quevedo-Teruel, M. Ebrahimpouri, and F. Ghasemifard, "Lens antennas for 5g communications systems," *IEEE Communications Magazine*, vol. 56, no. 7, pp. 36–41, 2018.

[22] M. Ebrahimpouri and O. Quevedo-Teruel, "Bespoke lenses based on quasi-conformal transformation optics technique," *IEEE Transactions on Antennas and Propagation*, vol. 65, no. 5, pp. 2256–2264, 2017.

[23] A. B. Numan, J.-F. Frigon, and J.-J. Laurin, "Printed *w*-band multibeam antenna with luneburg lens-based beamforming network," *IEEE Transactions on Antennas and Propagation*, vol. 66, no. 10, pp. 5614–5619, 2018.

[24] M. Bosiljevac, M. Casaletti, F. Caminita, Z. Sipus, and S. Maci, "Non-uniform metasurface luneburg lens antenna design," *IEEE transactions on antennas and propagation*, vol. 60, no. 9, pp. 4065–4073, 2012.

[25] K. Sato and H. Ujiie, "A plate luneberg lens with the permittivity distribution controlled by hole density," *Electronics and Communications in Japan (Part I: Communications)*, vol. 85, no. 9, pp. 1–12, 2002.

[26] O. Lafond, M. Himdi, H. Merlet, and P. Lebars, "An active reconfigurable antenna at 60 ghz based on plate inhomogeneous lens and feeders," *IEEE Transactions on Antennas and Propagation*, vol. 61, no. 4, pp. 1672–1678, 2012.

[27] A. Hessel, M. H. Chen, R. C. Li, and A. A. Oliner, "Propagation in periodically loaded waveguides with higher symmetries," *Proceedings of the IEEE*, vol. 61, no. 2, pp. 183–195, 1973.

[28] O. Dahlberg, R. Mitchell-Thomas, and O. Quevedo-Teruel, "Reducing the dispersion of periodic structures with twist and polar glide symmetries," *Scientific Reports*, vol. 7, no. 1, p. 10136, 2017.

[29] O. Quevedo-Teruel, M. Ebrahimpouri, and M. N. M. Kehn, "Ultrawideband metasurface lenses based on off-shifted opposite layers," *IEEE Antennas and Wireless Propagation Letters*, vol. 15, pp. 484–487, 2015.

[30] O. Luukkonen, C. Simovski, G. Granet, G. Goussetis, D. Lioubtchenko, A. V. Raisanen, and S. A. Tretyakov, "Simple and accurate analytical model of planar grids and high-impedance surfaces comprising metal strips or patches," *IEEE Transactions on Antennas and Propagation*, vol. 56, no. 6, pp. 1624–1632, 2008.

[31] M. G. Silveirinha, C. A. Fernandes, and J. R. Costa, "Electromagnetic characterization of textured surfaces formed by metallic pins," *IEEE Transactions on Antennas and Propagation*, vol. 56, no. 2, pp. 405–415, 2008.